

Received 13 September 2023, accepted 7 October 2023, date of publication 16 October 2023, date of current version 2 November 2023.

Digital Object Identifier 10.1109/ACCESS.2023.3325197

## RESEARCH ARTICLE

# Feasibility of Manufacturing Dielectric Image Lines by Using Laser-Based Directed Energy Deposition of Polymers

ALEXANDER WITTMANN<sup>1,2</sup>, TOBIAS BADER<sup>3</sup>, (Graduate Student Member, IEEE),  
SAEED ALIDOUST CHAMANDANI<sup>1</sup>, OLIVER HENTSCHEL<sup>1,2</sup>, MICHAEL SCHMIDT<sup>1,2</sup>,  
AND GERALD GOLD<sup>3</sup>, (Member, IEEE)

<sup>1</sup>Institute of Photonic Technologies (LPT), Friedrich-Alexander-Universität Erlangen-Nürnberg, 91052 Erlangen, Germany

<sup>2</sup>Erlangen Graduate School in Advanced Optical Technologies (SAOT), 91052 Erlangen, Germany

<sup>3</sup>Institute of Microwaves and Photonics, Friedrich-Alexander-Universität Erlangen-Nürnberg, 91058 Erlangen, Germany

Corresponding author: Alexander Wittmann (alexander.wittmann@lpt.uni-erlangen.de)

This work was funded by the Deutsche Forschungsgemeinschaft (DFG, German Research Foundation) under Project 411532653.


**ABSTRACT** The laser-based directed energy deposition of polymers (DED-LB/P) is an additive manufacturing process which offers the possibility to build up 3D structures with a high level of individualization on free-form surfaces. In this article, an absorber free DED-LB/P process with a thulium-doped fiber laser is presented for the first time to produce dielectric image lines (DIL) consisting of polypropylene (PP) for high frequency applications. This type of transmission line has advantages over the commonly used stripline technology due to its low signal attenuation, especially at high frequencies, but is currently hardly found in mass-market applications because no suitable manufacturing technology has been established for it yet. The steadily increasing demand of higher bandwidth in telecommunication or increased resolution of radar sensors leads to higher application frequencies and alternative interconnect technologies will become more important as they significantly define the achievable overall system performance. Based on the fabricated low-loss DILs in this study, DED-LB/P could represent such an alternative manufacturing process for future RF-applications.

**INDEX TERMS** Additive manufacturing, dielectric image lines, directed energy deposition, laser polymer deposition.

## I. INTRODUCTION

The ever growing need for higher bandwidth and therefore higher frequencies in the field of radio frequency (RF) circuits and communication pushes established technologies to their limits. Restrictions on freedom of spatial design and high losses in microstrip lines and other planar transmission lines are a huge obstacle and reach values of over 1.37 dB/cm [1] at frequencies higher than 100 GHz. Low loss transmission lines for high frequency application can only be formed by a dielectric strip, e.g. with a circular or rectangular cross

section. Since electromagnetic fields are also present in the immediate surroundings of this dielectric waveguide, a certain distance must be maintained by design, strongly limiting the possibilities of integrating them with other assembly and interconnect technologies. Since the electric field distribution of the propagation mode has a symmetry plane, a ‘mirror’ can be introduced at this plane without changing propagation properties of the transmission line [2], [3]. A perfect mirror would be a sheet showing infinite conductivity and an ideally smooth surface. Practical realization with a conductive sheet affects the propagation properties of the transmission lines due to conductor loss and inner inductance, which heavily depend on the surface profile.

The associate editor coordinating the review of this manuscript and approving it for publication was Jingang Jiang .

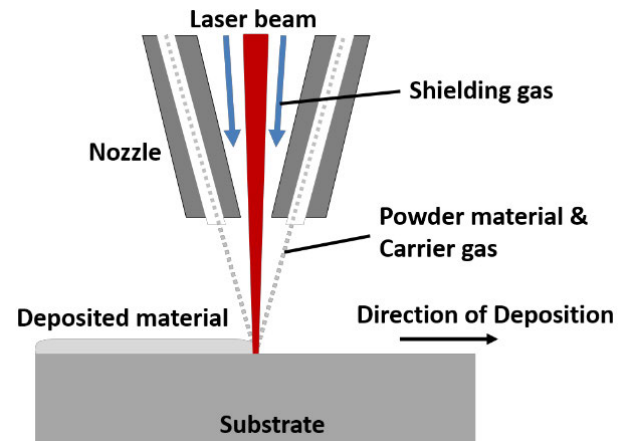
**TABLE 1. Attenuation of established transmission lines in W-band.**

Line Type	Attenuation dB/m	Reference
Coplanar waveguide	130.35	[4]
Microstrip	136.93	[1]
Hollow waveguide	2.63	[5]
Dielectric waveguide	1.80	[6]

In the regarded frequency range above 100 GHz planar transmission lines, e.g. microstrip lines or coplanar waveguides already show very high attenuation, whereas hollow waveguides and dielectric waveguides have significantly lower losses (see Tab. 1 for typical figures) but usually are difficult to integrate. Thus, a DIL can be considered as a compromise between the achievable transmission properties and integrability.

The concept of DILs is well known [7], [8] and it is widely accepted as a promising type of transmission line. Theoretically, the signal attenuation of a DIL can be lower than hollow waveguides and its planar structure could be used in a wide range of applications. The lack of industrial application can be regarded as the result of a missing automated manufacturing process. In laboratory applications, the DIL is manufactured by subtractive machining and subsequently gluing the dielectric onto a metallic substrate [3]. In order to address the aforementioned challenges, DED-LB/P represents a promising approach for fabricating DILs. DED-LB/P is an additive manufacturing process, in which a laser beam is used to melt a polymeric feedstock as it is being deposited [9]. A schematic representation of the DED-LB/P process using powder feedstock material is shown in Fig. 1. Analogous to the laser-based directed energy deposition of metals (DED-LB/M), DED-LB/P offers the possibility to build up 3D parts on free-form surfaces through line-by-line deposition [10]. As near-net shapes are created directly from computer aided design data, a shortening of the process chain can be reached compared to conventional manufacturing processes. In addition, complex functional gradients, multi-material structures and composite materials with tailored properties can be fabricated by using a multi-hopper powder feeder [11].

Despite the above-mentioned advantages, DED-LB/P has been investigated only to a limited extent in literature so far. In order to enhance the wear-resistance of elastomers in sealing and sliding systems, polyamide 11 (PA11) and thermoplastic polyurethane (TPU) based coatings were applied by DED-LB/P in previous studies [12], [13]. Results show a substantial reduction of the frictional forces by the deposited PA11 coatings compared to the elastomer substrates. In particular, the admixture of polytetrafluoroethylene and molybdenum disulfide powders to the feedstock was a purposeful approach [12], [13]. In addition to the consolidation of functional coatings, building up 3D parts by DED-LB/P was demonstrated in previous studies [14], [15], [16]. The fabricated polyamide 12 (PA12) [14], [15] and TPU [16] structures indicate a high level of

**FIGURE 1. Simplified illustration of the DED-LB process using powder feedstock material.**

roughness and poor mechanical properties, which are attributed to partially molten particles and a high porosity. Furthermore, an important point to note is that common near-infrared (NIR) laser beam sources in the wavelength range between 0.9  $\mu\text{m}$  and 1.1  $\mu\text{m}$  were used in the aforementioned studies about DED-LB/P. As polymers exhibit a high transparency in this wavelength range, the thermoplastic feedstocks were modified with additives (carbon black [12], [16], multi-walled carbon nanotubes [14], [15]) to ensure a sufficient laser absorption. However, the addition of these additives affects the transmission properties of DILs, which inhibits the use in millimeter wave applications. In summary, further developments are necessary at both material and process level to establish DED-LB/P as a competitive additive manufacturing process.

Instead of modifying the polymer system with absorbing additives, the laser beam source can be adjusted to reach suitable absorption characteristics during DED-LB/P processing. Based on previous studies in literature [17], [18], it is expected that CO<sub>2</sub> lasers are only partially suitable in DED-LB/P. Due to the low optical penetration depth in the polymer powder, the interface between substrate and deposited layer cannot be heated sufficiently. In addition, the laser radiation of a CO<sub>2</sub> laser cannot be guided through glass fibers, which makes the integration into a DED-LB/P setup more difficult than with NIR laser beam sources [16].

Since most thermoplastic polymers exhibit characteristic absorption bands at wavelengths above 1.5  $\mu\text{m}$  [19], the use of a thulium-doped fiber laser system with a wavelength of around 2  $\mu\text{m}$  is an interesting approach in DED-LB/P. Laumer et al. [20] measured at a wavelength of 1.94  $\mu\text{m}$  the optical properties of thermoplastic powders with an experimental setup consisting of two integration spheres. PA12 powder layers with a thickness of 200  $\mu\text{m}$  show an absorptance of 31%, a reflectance of 40% and a transmittance of 29%. Based on the optical characteristics of the polymer powder, a thulium-doped fiber laser with a wavelength of 1.94  $\mu\text{m}$  was investigated in an absorber-free

DED-LB/P process. The suitability of this laser beam source was proven by producing single-layer PA12 coatings with low porosity (2.3 %) and good adhesion on the stainless steel substrates [21].

In the present manuscript, DED-LB/P is investigated for the first time to additively manufacture polymer-based DILs for microwave applications. It is assumed, that an absorber-free DED-LB/P process with a thulium-doped fiber laser is appropriate to fabricate low-loss DILs. PP powder is used for fabricating the DILs due to a suitable loss tangent of about  $2 \cdot 10^{-3}$  and a relative permittivity of around 2.2. These values were measured with a cavity resonator up to 36 GHz. As reported in [3], a DIL with rectangular cross section, made from a dielectric with a relative permittivity of 2.2 should have dimensions of about 1.8 mm times 0.9 mm for W-Band applications. Unlike presented in [2] and [3], DILs with a semi-elliptical cross section are fabricated in this study. This geometry is much easier to realize in DED-LB/P than rectangular cross sections. The change of the geometry has no obvious disadvantages except that the DIL does not fit perfectly into the wave mode transition presented in this paper. In order to evaluate the potential of DED-LB/P for producing DILs, the generated PP structures are analyzed with regard to the geometrical dimensions, porosity, surface roughness, shear strength and transmission properties. In this context, the DILs are characterized for a frequency range from 75 GHz to 110 GHz (W-band) to exemplify the application and possibilities of this type of line for frequency bands above 100 GHz.

## II. MANUFACTURING OF DIELECTRIC IMAGE LINES

Due to a low dielectric loss factor, PP powder (AM Polymers, Willich, Germany) with an average particle size ( $x_{50,3}$ ) of  $81.6 \pm 3.2 \mu\text{m}$  was used to fabricate the DIL by DED-LB/P. A fiberglass-reinforced epoxy-laminated sheet (FR4) with a copper coating of  $35 \mu\text{m}$  thickness (Bungard, Windeck, Germany) was selected exemplarily as substrate material for the experimental investigations. In order to improve the mechanical interlocking between the substrate and deposited PP structures, the copper surfaces were sandblasted (SM 2002 A, HGH, Lüdenscheld, Germany) using a microblasting system (HGH 6040, HGH, Lüdenscheld, Germany). All substrates were cleaned with ethanol to remove residues of the sandblasting process. The average roughness ( $R_a$ ) of the sandblasted surfaces was determined as  $7.96 \pm 0.98 \mu\text{m}$ .

The experimental DED-LB/P setup in this study for fabricating the DILs is schematically shown in Fig. 2. A single-mode thulium-doped fiber laser system (TLR-120, IPG, Burbach, Germany) with a wavelength of  $1.94 \mu\text{m}$  and a maximum output power of 120 W was used. The laser beam with a Gaussian profile was guided by the laser processing head (YC30, Precitec, Gaggenau, Germany) onto the substrate surface. The relative movement between the laser processing head and the substrate was realized by a positioning system (Aerotech, Fürth, Germany) with a three translational axis. The powder feed to the four-jet

**TABLE 2.** Experimental design for the fabrication of DILs by DED-LB/P.

Parameter Set	1	2
Substrate temperature ( $^{\circ}\text{C}$ )	23	100
Laser power 1st layer (W)	34	27
Laser power 2nd – 6th layer (W)	27	27
Dwell time (s)	1	8
Feed rate (mm/s)		10
Beam diameter (mm)		1.9
Carrier gas flow (L/min)		6
Shielding gas flow (L/min)		10
Working distance (mm)		14
Powder mass flow (g/min)		0.5

**TABLE 3.**  $R_a$  of the weld tracks with five layers.

Parameter Set	$R_a$
1	$30.47 \pm 0.80 \mu\text{m}$
2	$24.99 \pm 1.21 \mu\text{m}$

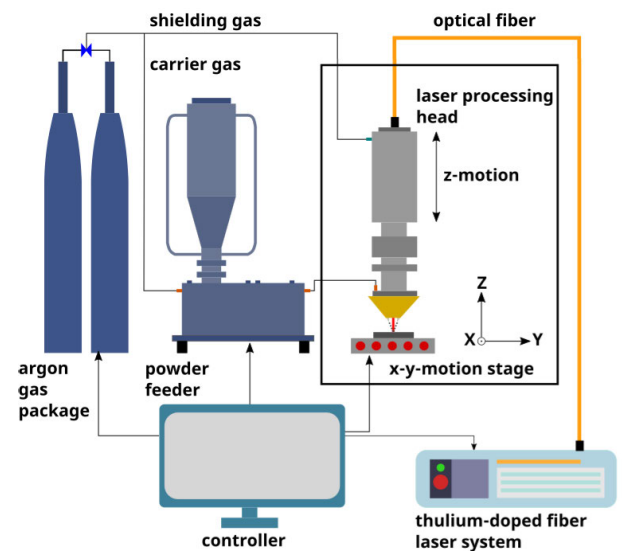


**FIGURE 2.** Schematic of the DED-LB/P setup for the fabrication of DILs on metallic substrates [21].

nozzle of the laser processing head was implemented using a vibrating powder feeder (Flowmotion, Medicoat, Wohlen, Switzerland). Argon was used as carrier and shielding gas for preventing oxidative degradation mechanism of the polymer powder. A hot plate with a maximum temperature of  $150^{\circ}\text{C}$  was integrated into the experimental setup to heat the substrate plate.

In order to realize the DILs for RF applications, 3D structures with a semi-elliptical cross section were fabricated with DED-LB/P. For this purpose, welding tracks with a length of 30 mm were applied on the copper surfaces. Up to six layers were deposited by an alternating scan strategy to reach appropriate heights of the DIL. The DED-LB/P process was stopped between each layer for a certain period (dwell time) to avoid excessive heat accumulations. Table 2 presents two optimized parameter sets for generating homogeneous structures on the substrate surfaces. As excessive melt pool temperatures can cause process instabilities during DED-LB/P processing [21], the energy input was tailored by varying the substrate temperature, laser power and delay time. The remaining parameters (feed rate, beam diameter, powder

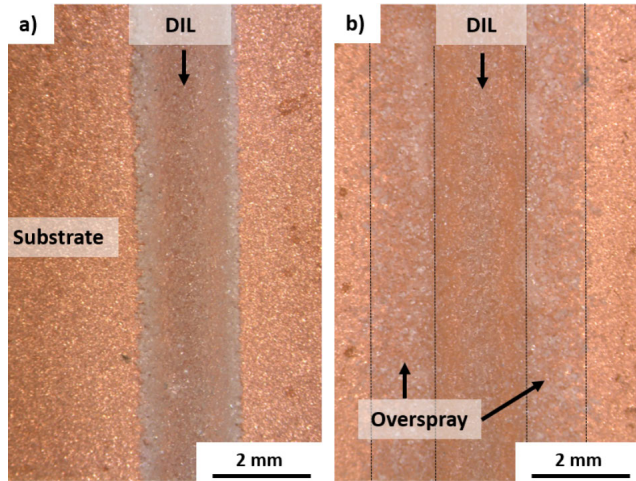


FIGURE 3. Microscopic image of the sample surface processed by (a) parameter set 1 and (b) set 2.

TABLE 4. Maximum shear forces and shear stresses of the samples with five layers (n = 3).

Parameter Set	Maximum shear force N	Shear strength MPa
1	10.4 ± 2.0	0.14 ± 0.03
2	21.8 ± 3.9	0.19 ± 0.03

mass flow, carrier gas flow, shielding gas flow and working distance) were kept constant.

### III. CHARACTERIZATION OF THE GENERATED STRUCTURES

Microscopic images (M80, Leica, Wetzlar, Germany) of the sample surface generated by set 1 and set 2 are shown in Fig. 3. For the samples processed by set 1 a sharp distinction between the substrate and DIL is recognizable. By contrast, an overspray on the substrate can be seen for samples produced by set 2. Due to elevated substrate temperature of 100 °C, the adhesion of powder particles to the substrate is promoted in close proximity to the laser-material interaction zone.

DILs built up by set 1 exhibit a tendency towards lifting at the corners and thus a localized delamination from the copper surface. Thermally induced residual stresses due to non-uniform temperature gradients are implicated as the underlying cause. Analogous to laser-based powder bed fusion of polymers (PBF-LB/P), the deformation of the generated DILs caused by a fast or an inhomogeneous crystallization have to be considered [22]. As a consistent adhesion of the DIL on the substrate is observed for set 2, it is assumed that the residual stresses are reduced sufficiently at a substrate temperature of 100 °C.

A 3D optical profilometer (VR-6000, Keyence, Osaka, Japan) was used to measure the geometrical dimensions of the fabricated DILs. Fig. 4 shows the cross section of a five-layer structure deposited by set 1 and set 2. On the basis of the cross-sectional dimensions, the height (Fig. 5) and width of the DILs (Fig. 6) depending on the number of deposited layers were determined. DIL heights in the range from 0.17 ±

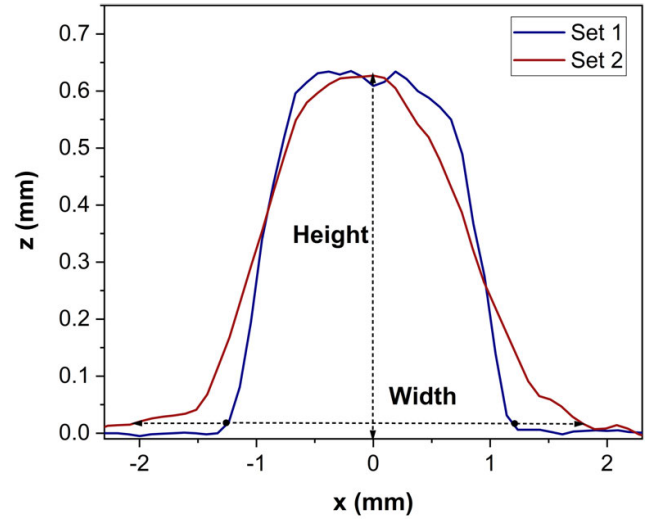


FIGURE 4. Cross-sectional geometry of a five-layer DIL deposited by set 1 and set 2.

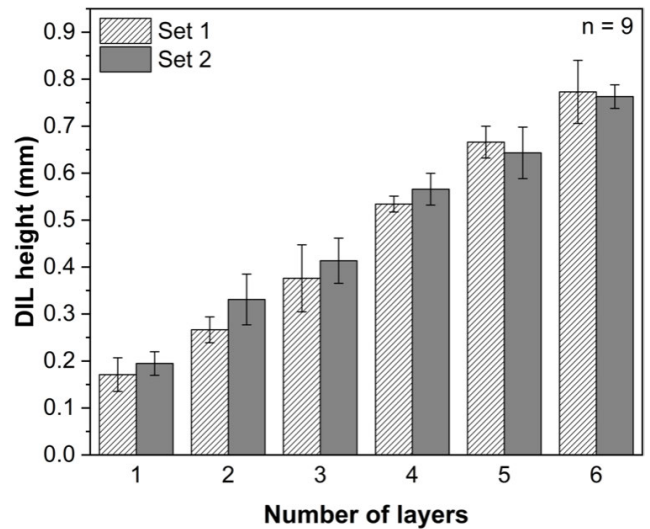
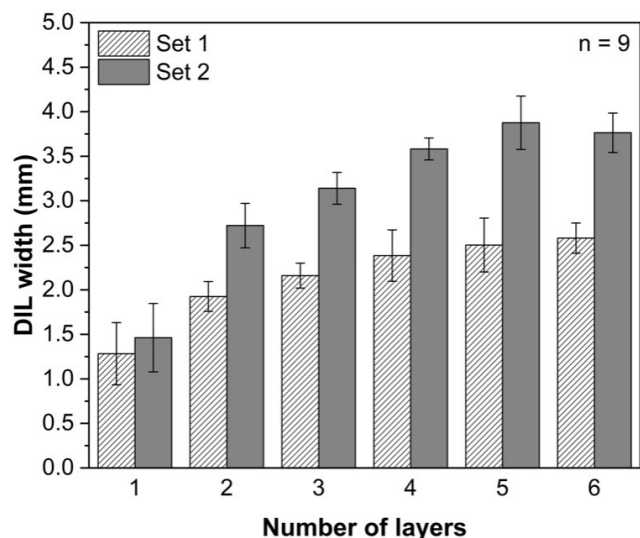


FIGURE 5. DIL height as a function of the number of layers for set 1 and set 2.

0.04 mm to 0.76 ± 0.03 mm can be achieved by adapting the number of layers. When comparing the two parameter sets, no significant differences are evident with regard to the DIL height. The DILs deposited by set 1 and set 2 show a maximum width of 2.58 ± 0.17 mm and 3.88 ± 0.30 mm, respectively. The higher DIL widths of set 2 compared to set 1 are attributed to the positive effect of a substrate heating on the wetting behavior [23].

Cross sections of the DILs were prepared using a disc cutting machine (Discotom-10, Struers, Willich, Germany) and subsequently grinded as well as polished. The generated cross sections were analyzed in terms of possible defects by optical microscopy (BX53M, Olympus, Tokyo, Japan). In order to quantify the porosity of the DILs, the open-source image processing software ImageJ was used. The microscopic images (Fig. 7) show a clear differentiability between set 1 and set 2 with regard to porosity. Compared to set 2, pores with much larger diameters (188 ± 95 μm to 367 ±



**FIGURE 6.** DIL width as a function of the number of layers for set 1 and set 2.

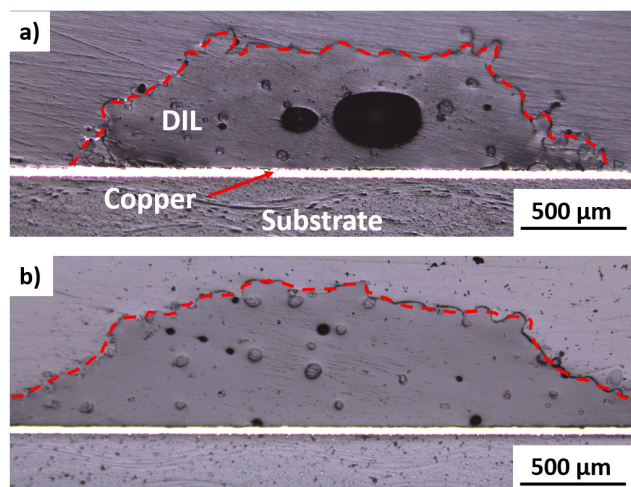


**FIGURE 7.** Exemplary microscopic images of polished cross sections of DILs with five layers fabricated by a) set 1 and b) set 2.

62  $\mu\text{m}$ ) are striking for set 1. While a porosity of  $0.7 \pm 0.1\%$  is reached for DILs fabricated by set 2, a porosity up to  $8.1 \pm 2.9\%$  can be seen for set 1.

The arithmetical average roughness ( $R_a$ ) was analyzed with a confocal laser scanning microscope (LEXT 4000, Olympus) longitudinally on the DIL. Thereby, the measurements were performed within the center along the peak of the DILs. DILs with five layers were characterized exemplarily to determine  $R_a$ . According to DIN EN ISO 4288, a cut-off wavelength ( $\lambda_c$ ) of 8 mm was selected. In general, the fabricated DILs reveal high  $R_a$  values (Table 3). A comparison of the two parameter sets presents a 20% lower  $R_a$  value of the DILs deposited by set 2. The reduced density and roughness of 3D structures fabricated by set 2 can generally be associated with an improved coalescence of the polymer particles. Due to the lower cooling rate induced by the heating of the substrate, rapid

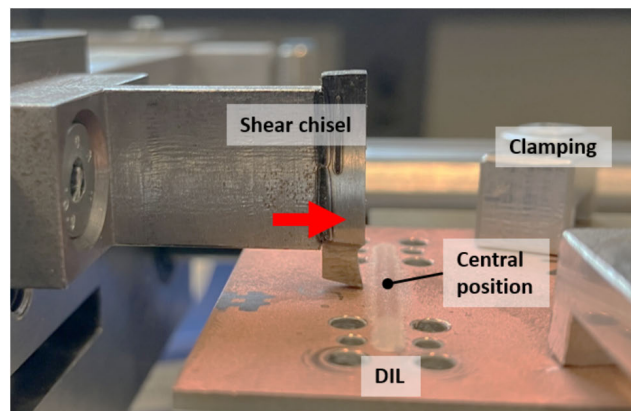


**FIGURE 8.** Experimental setup for the shear tests.

solidification of the polymer can be avoided, thus extending the duration of the molten phase.

In order to investigate the influence of the process parameters on the shear strength between DIL and substrate, shear tests were carried out. For this purpose, the substrates were positioned and fixed in the shear test rig, as shown in Fig. 8. The DIL structures were then sheared off with a chisel moving at a speed of 0.05 mm/s. The forces acting during the shear process were recorded with a 100 N load cell (KD40s, ME-Messsysteme, Hennigsdorf, Germany). The corresponding shear strength was calculated by using the bonding surface between the DIL and substrate. It is well-known from machining that the chisel edge can influence the shear strength [24]. Therefore, it is important to mention that a comparison of the determined shear strengths with literature values is only possible to a limited extent. Table 4 presents the determined maximum shear forces and shear strengths for samples with five layers. A comparison of both parameter sets shows a 35.7% higher shear strength for the samples produced by set 2. The adhesion between the DIL and the substrate could be attributed to an interplay of adsorption theory, weak-boundary-layer theory and mechanical theory [23], [25]. Since the substrate surface is roughened by sandblasting, the mechanical interlocking between the DIL and the substrate is a significant factor for the adhesion. The increased bond strength caused by a substrate heating is in accordance with previous studies in literature [26], [27]. Due to the improved wetting at elevated substrate temperatures, a large active area for intermolecular interaction and hence a higher strength is ensured [27].

#### IV. ELECTRICAL MEASUREMENTS

To acquire the transmission characteristics, a back-to-back measurement setup, like shown in Fig. 9 is used. For this setup two 3D-printed and subsequently metal plated transitions from WR-10 waveguides to the DIL are used. These transitions are screwed onto the substrate, like shown in Fig. 10. It is important to note, that these transitions were designed for a DIL with rectangular cross section and tapered DILs [3]. The geometrical dimensions of these transitions are shown in Fig. 11 and described in Tab 5. Each transition has

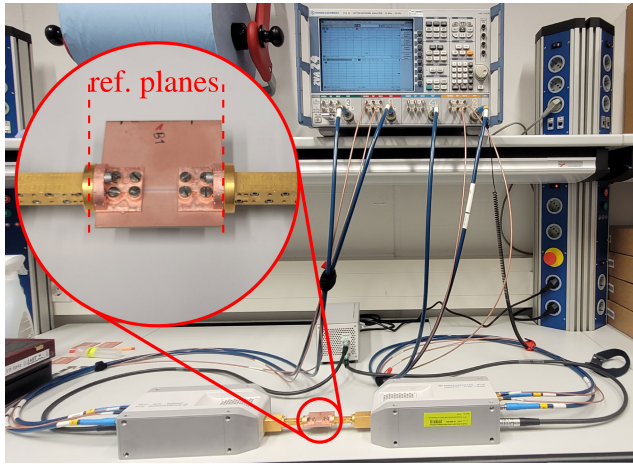


FIGURE 9. Back-to-back-setup to measure the S-parameters.

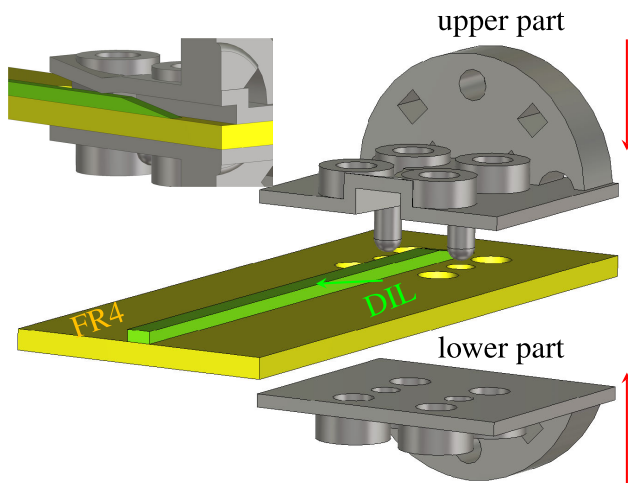


FIGURE 10. Exploded-view drawing and cross section of the used waveguide to DIL transition.

three segments. After a short section of a hollow waveguide (A), the transition to a dielectrically filled waveguide is achieved by narrowing the cross section in (B) and finally, a horn like widening in (C) assures matching to the DIL.

To characterize the transmission capabilities of the produced specimens measurements with a Rohde & Schwarz ZVA-24 are performed. It is calibrated with a standard TOSM-calibration, which sets the reference planes to the measurement flanges (Fig. 9). Due to the high complexity of the DED-LB/P process, it must be considered that this study is focused on the production of DILs with a constant length (30 mm). Increasing the length of the DILs poses a challenge regarding the adhesion on the substrate, which should be investigated in future work. As a consequence, the wave mode transitions are not de-embedded.

The measured S-Parameters of the produced sets 1 and 2 for a number of 5 layers and over a frequency range from 75 GHz to 110 GHz are shown in Fig. 12 and 13. It is clearly evident that the specimens which show overspray (set 2), due to a heated build platform, perform worse than the ones without (set 1). As mentioned, the transition was not designed for the resulting cross section. Consequently, a powder

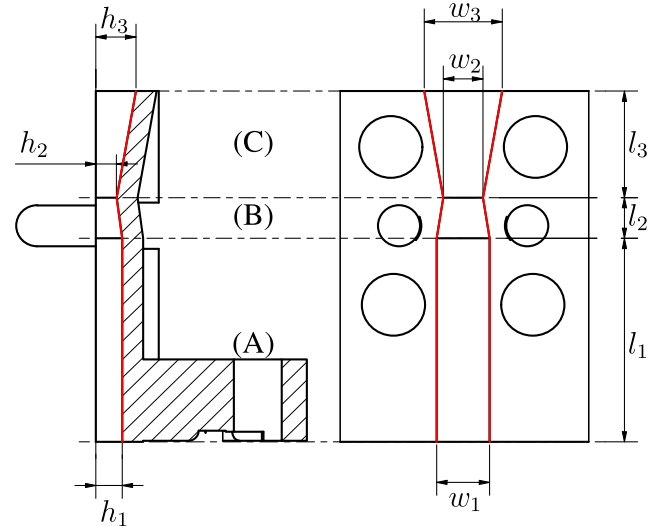


FIGURE 11. Dimensions of the waveguide to DIL transition.

TABLE 5. Geometric dimensions of the mode transition shown in Fig. 11.

Segment Parameter	1	2	3
h (mm)	1.27	1.00	1.92
l (mm)	10.00	2.00	5.24
w (mm)	2.54	1.9	3.75

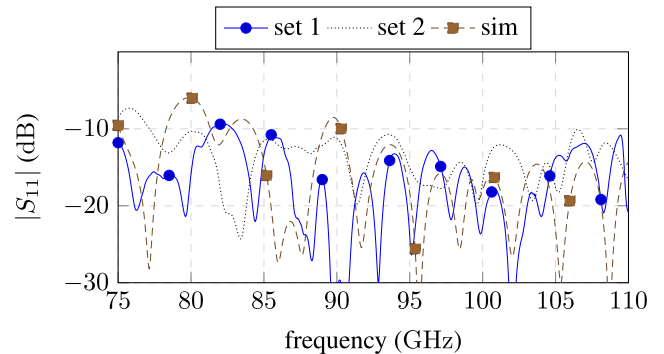


FIGURE 12.  $|S_{11}|$  of sets 1 and 2 and the simulation.

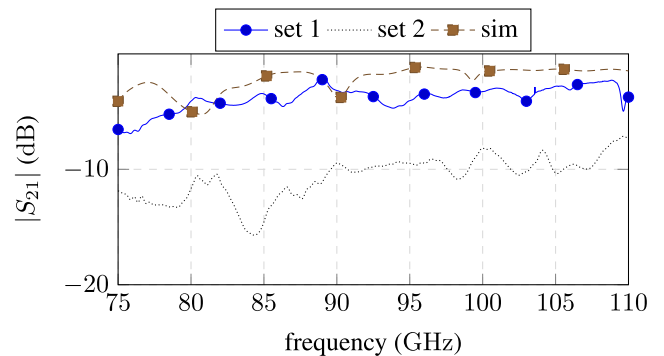
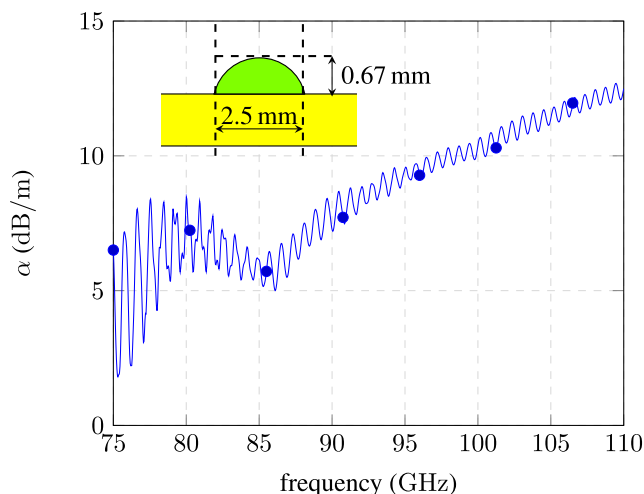


FIGURE 13.  $|S_{21}|$  of the sets 1 and 2 and of the simulation.

overspray in set 2 worsens the performance significantly compared to set 1. The measured reflection loss for set 1 shows values under 10 dB almost throughout the frequency range. Set 1 also has an acceptable insertion loss reaching from  $-7.85$  dB to  $-3.57$  dB.



**FIGURE 14.** Simulated damping coefficient  $\alpha$  of the DIL with the used crosssection.

On the basis of the measured geometrical dimensions (Fig. 5, Fig. 6) of the produced DIL, the S-parameters were simulated. Note that, for this simulation the relative permittivity of the printed PP was estimated to be 2.2 at 90 GHz, although the DED-LB/P process produces DILs with pores which can be seen in Fig. 7. Also the measured average surface roughness of the substrate ( $R_a$ ) was taken into account. Despite the determined porosity, the simulations seen in Fig. 12 and Fig. 13 show an adequate agreement with the measured data.

Due to the aforementioned constant length of the produced DILs, multi line measurement could not be performed. However, a simulative estimation of the line loss itself was carried out using a multiline method [28] to obtain the damping coefficient of the transmission line without influence from the waveguide transitions. The estimated damping coefficient  $\alpha$  is plotted in Fig. 14 and shows a maximum attenuation of 13 dB/m, which is a great improvement compared to typical planar transmission lines. Therefore, the feasibility of producing low-loss DILs with the help of DED-LB/P was demonstrated.

## V. CONCLUSION

A dielectric image line would be superior to conventional planar striplines in terms of attenuation, yet it is rarely found in any application due to a lack of an automated manufacturing process. In this work, an absorber-free DED-LB/P process with a thulium-doped fiber laser is presented to produce DILs for microwave applications. The produced specimens reached a reflection loss of 10 dB in nearly the entire W-band and a maximum insertion loss of 7.85 dB, whereas simulations with parameters based on the experiments indicate line losses alone with a maximum of 0.13 dB/cm. Compared to a microstrip line with a line loss of around 1.37 dB/cm this is a good and promising improvement. Since substrate heating improves the shear strength of the applied DILs on the one hand and negatively affects the transmission characteristics on the other, a compromise must be found depending on the requirements of the RF application. Therefore, further

investigation should be performed on the manufacturing parameters and on possible pretreatments of the substrate surface to improve adhesion as well as electrical performance of the DIL. Also, the wavemode transducers used to connect hollow waveguides to the DIL have to be redesigned to fit to the process specific cross section of the DIL. Overall the performed attempts give reason for confidence, that the DED-LB/P process is a manufacturing technology capable of producing the necessary basic components of a new alternative assembly and interconnect for future applications operating at frequencies > 100 GHz. The 3D capability and its achievable feature sizes together with the variety of usable polymers enable e.g. new antenna in package concepts or broadband chip to chip connections.

## ACKNOWLEDGMENT

The authors want to thank the Deutsche Forschungsgemeinschaft (DFG, German Research Foundation) for funding the project “Flexible fabrication of functional integrated coatings and structures for the reconstructive medicine using laser cladding of PEEK” (Project number 411532653). We gratefully thank Christian Staudenmaier (Precitec GmbH & Co. KG) for providing the laser processing head (YC30) free of charge. We also thank Sven Ackermann (Robert Bosch GmbH) for size measurements of the polymer powder particles via Camsizer X2 and Julian Schrauder (Bayerisches Laserzentrum GmbH) for assistance with shear tests. The authors gratefully acknowledge funding of the Erlangen Graduate School in Advanced Optical Technologies (SAOT) by the Bavarian State Ministry for Science and Art. We acknowledge financial support by Deutsche Forschungsgemeinschaft and Friedrich-Alexander-Universität Erlangen-Nürnberg within the funding program “Open Access Publication Funding”.

## REFERENCES

- [1] D. M. Pozar, *Microwave Engineering*, 4th ed. Hoboken, NJ, USA: Wiley, 2012.
- [2] I. Wolff and K. Solbach, *Dielectric Image Lines*. Aachen, Germany: Verlagsbuchhandlung Dr. Wolff GmbH, 2020.
- [3] H. Tesmer, D. Stumpf, E. Polat, D. Wang, and R. Jakoby, “Dielectric image line rod antenna array with integrated power divider at W-band,” in *Proc. 16th Eur. Conf. Antennas Propag. (EuCAP)*, Madrid, Spain, Mar. 2022, pp. 1–5.
- [4] O. Huber, T. Faseth, G. Magerl, and H. Arthaber, “Dielectric characterization of RF-printed circuit board materials by microstrip transmission lines and conductor-backed coplanar waveguides up to 110 GHz,” *IEEE Trans. Microw. Theory Techn.*, vol. 66, no. 1, pp. 237–244, Jan. 2018.
- [5] K. Lomakin, G. Gold, and K. Helmreich, “Transmission line model for rectangular waveguides accurately incorporating loss effects,” in *Proc. IEEE 21st Workshop Signal Power Integrity*, Lake Maggiore, Italy, May 2017, pp. 1–4.
- [6] F. Distler, M. Vossiek, and J. Schür, “Novel dielectric waveguide design studies for mmW applications,” in *Proc. Asia-Pacific Microw. Conf. (APMC)*, Nov. 2018, pp. 288–290.
- [7] D. D. King, “Dielectric image line,” *J. Appl. Phys.*, vol. 23, no. 6, pp. 699–700, Jun. 1952.
- [8] D. D. King and S. P. Schlesinger, “Dielectric image lines,” *IEEE Trans. Microw. Theory Techn.*, vol. MTT-6, no. 3, pp. 291–299, Jul. 1958.
- [9] I. Gibson, D. Rosen, and B. Stucker, *Additive Manufacturing Technologies: 3D Printing, Rapid Prototyping, and Direct Digital Manufacturing*. New York, NY, USA: Springer, 2015.

- [10] D.-G. Ahn, "Directed energy deposition (DED) process: State of the art," *Int. J. Precis. Eng. Manuf.-Green Technol.*, vol. 8, no. 2, pp. 703–742, Mar. 2021.
- [11] D. Dev Singh, S. Arjula, and A. Raji Reddy, "Functionally graded materials manufactured by direct energy deposition: A review," *Mater. Today, Proc.*, vol. 47, pp. 2450–2456, 2021.
- [12] M. Rombouts, A. Vanhulsel, A. Komp, J. Gedopt, W. Engelen, and R. Persoons, "Production of low-friction coatings by laser cladding," in *Proc. Int. Congr. Appl. Lasers Electro-Opt.*, Temecula, CA, USA, 2008, p. 2101.
- [13] B. Verheyde, M. Rombouts, A. Vanhulsel, D. Havermans, J. Meneve, and M. Wangenheim, "Influence of surface treatment of elastomers on their frictional behaviour in sliding contact," *Wear*, vol. 266, nos. 3–4, pp. 468–475, Feb. 2009.
- [14] Y. Kutlu, Y. L. Wencke, G. A. Luinstra, C. Esen, and A. Ostendorf, "Directed energy deposition of PA12 carbon nanotube composite powder using a fiber laser," *Proc. CIRP*, vol. 94, pp. 128–133, Jan. 2020.
- [15] Y. L. Wencke, Y. Kutlu, M. Seefeldt, C. Esen, A. Ostendorf, and G. A. Luinstra, "Additive manufacturing of font-variant: PA12 carbon nanotube composites with a novel laser polymer deposition process," *J. Appl. Polym. Sci.*, vol. 138, p. 50395, May 2021.
- [16] M. Thiele, Y. Kutlu, H. Dobbelsstein, M. Petermann, C. Esen, and A. Ostendorf, "Direct generation of 3D structures by laser polymer deposition," *J. Laser Appl.*, vol. 33, no. 2, May 2021, Art. no. 022002.
- [17] C. Zhang, G. Zhang, Y. Ji, H. Liao, S. Costil, and C. Coddet, "Microstructure and mechanical properties of flame-sprayed PEEK coating remelted by laser process," *Prog. Organic Coat.*, vol. 66, no. 3, pp. 248–253, Nov. 2009.
- [18] M. Dahmen, C. Vedder, S. Baek, and J. Stollenwerk, "Dual-beam laser-based processing of tribological polymer coatings," *Proc. CIRP*, vol. 111, pp. 257–260, Jan. 2022.
- [19] M. Brosda, P. Nguyen, A. Olowinsky, and A. Gillner, "Laserwelding of biopolymers," *Proc. CIRP*, vol. 74, pp. 548–552, Jan. 2018.
- [20] T. Laumer, T. Stichel, K. Nagulin, and M. Schmidt, "Optical analysis of polymer powder materials for selective laser sintering," *Polym. Test.*, vol. 56, pp. 207–213, Dec. 2016.
- [21] A. Wittmann, O. Hentschel, A. Sommereyns, and M. Schmidt, "Generation of polyamide 12 coatings on stainless steel substrates by directed energy deposition with a thulium-doped fiber laser (DED-LB/P)," *Polymers*, vol. 14, no. 18, p. 3729, Sep. 2022.
- [22] M. Schmid, *Laser Sintering With Plastics: Technology, Processes, and Materials*, 1st ed. Cincinnati, OH, USA: Hanser Publishers, 2018.
- [23] H. Sändker, "Laserbasierte herstellung funktionaler beschichtungen aus partikulärem polyetheretherketon," Ph.D. thesis, RWTH Aachen Univ., Aachen, Germany, 2018. [Online]. Available: <http://publications.rwth-aachen.de/record/753549>
- [24] M. Gonzalez, A. Rodriguez, O. Pereira, A. Celaya, L. N. L. De Lacalle, and M. Esparta, "Axial-compliant tools for adaptive chamfering of sharp-edges: Characterisation and modelling," *Eng. Sci. Technol., Int. J.*, vol. 41, May 2023, Art. no. 101407.
- [25] L. F. M. Da Silva, A. Öchsner, and R. D. Adams, *Handbook of Adhesion Technology*. Berlin, Germany: Springer, 2011.
- [26] A. Wittmann, J. Heberle, F. Huber, and M. Schmidt, "Consolidation of thermoplastic coatings by means of a thulium-doped fiber laser," *J. Laser Appl.*, vol. 33, no. 4, Nov. 2021, Art. no. 042032.
- [27] M. Dahmen, C. Vedder, M. Speckens, J. Stollenwerk, and P. Loosen, "Influence of surface preheating and pretreatment on the adhesion of laser-melted PEEK to aluminum substrates," *Surf. Coat. Technol.*, vol. 448, Oct. 2022, Art. no. 128922.
- [28] R. B. Marks, "A multiline method of network analyzer calibration," *IEEE Trans. Microw. Theory Techn.*, vol. 39, no. 7, pp. 1205–1215, Jul. 1991.



**TOBIAS BADER** (Graduate Student Member, IEEE) received the B.Eng. degree in electronics and sensor technologies from the Karlsruhe University of Applied Science, in 2019, and the M.Sc. degree in electronics from Friedrich-Alexander-Universität Erlangen-Nürnberg (FAU), in 2022, where he is currently pursuing the Ph.D. degree with the Institute of Photonic Technologies. After his graduation, he joined the Institute of Microwaves and Photonics, FAU, as a Research Assistant. His current research interest includes the additive manufacturing of dielectric image lines and waveguides.



**SAEED ALIDOUST CHAMANDANI** received the B.Sc. degree from the Amirkabir University of Technology, in 2014, and the M.Sc. degree in biomedical engineering from the Khajeh Nasir Toosi University of Technology, in 2017. Since then, he worked in the fields of mechatronics and embedded systems as a research and development engineer, until 2021, when he joined the master's program in advanced optical technologies with Friedrich-Alexander-Universität Erlangen-Nürnberg. Currently, he is a Student Research Assistant with the Institute of Photonic Technologies. His current research interest includes optical technologies.



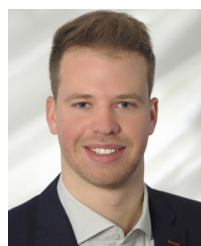
**OLIVER HENTSCHEL** received the Diploma degree in physical engineering and applied physics from the Coburg University of Applied Science, in 2008, and the M.Sc. degree in physical engineering and applied physics from the RheinMain University of Applied Science, in 2012. Since October 2012, he has been a Research Assistant with the Institute of Photonic Technologies, Friedrich-Alexander-Universität Erlangen-Nürnberg (FAU). His current research interests include additive manufacturing, in particular laser-based directed energy deposition (DED-LB/M) of nanoparticle-reinforced tool steels and composite materials.



**MICHAEL SCHMIDT** received the Ph.D. degree in process control of laser spot welding in electronics production, in 2002. Following his engagement in its executive board, he has been leading Bayerisches Laserzentrum GmbH as the Managing Director, since January 2005. He has been the Chair of the Institute of Photonic Technologies, Friedrich-Alexander-Universität Erlangen-Nürnberg, since it was founded, in 2009. His current research interests include laser applications from the micro- to macroscopic scale within the fields of industrial manufacturing, additive manufacturing, and medical engineering.



**GERALD GOLD** (Member, IEEE) received the Diploma and Dr.Eng. degrees in mechatronics from Friedrich-Alexander-Universität Erlangen-Nürnberg (FAU), Erlangen, Germany, in 2009 and 2016, respectively. He joined the Institute of Microwaves and Photonics, FAU, in 2010, as a Research Assistant, where he became the Group Leader of the Microwave Assembly and Interconnects Group, in 2018. His current research interests include 3D-printed RF components, material characterization, EM-interaction with non-ideal surfaces, and automation of RF measurements. He is a member of the IEEE MTT-S Technical Committee MTT-16.



**ALEXANDER WITTMANN** received the B.Sc. and M.Sc. degrees in materials science and engineering from the University of Bayreuth, in 2016 and 2019, respectively. He is currently pursuing the Ph.D. degree with the Institute of Photonic Technologies, Friedrich-Alexander-Universität Erlangen-Nürnberg (FAU). After his graduation, he joined Bayerisches Laserzentrum GmbH as a Project Engineer. Since August 2020, he has been a Research Assistant with the Institute of Photonic Technologies, FAU. His current research interest includes laser material processing of polymers and metals.

...